Energy and Environmental Science

ARTICLE

Hybrid capacitive deionization to enhance the desalination performance of capacitive techniques

Jaehan Lee,[a] Seoni Kim,[a] Choonsoo Kim[a] and Jeyong Yoon[a*]

Based on a porous carbon electrode, capacitive deionization (CDI) is a promising desalination technology in which ions are harvested and stored in an electrical double layer. However, the ion removal capacity of CDI systems is not sufficient for desalting high-concentration saline water. Here, we report a novel desalination technique referred to as "hybrid capacitive deionization (HCDI)", which combines CDI with a battery system. HCDI consists of a sodium manganese oxide ($Na_4Mn_9O_{18}$) electrode, an anion exchange membrane, and a porous carbon electrode. In this system, sodium ions are captured by the chemical reaction in the $Na_4Mn_9O_{18}$ electrode, whereas chloride ions are adsorbed on the surface of the activated carbon electrode during the desalination process. HCDI exhibited more than double the ion removal sorption capacity (31.2 mg/g) than a typical CDI system (13.5 mg/g). Moreover, it was found that the system has a rapid ion removal rate and excellent stability in an aqueous sodium chloride solution. These results thus suggest that the HCDI system could be a feasible method for desalting a highly concentrated sodium chloride solution in capacitive techniques.

Introduction

Capacitive deionization (CDI) is a desalination technology that removes ions from saltwater using electrical absorption and desorption on the surface of electrodes. It is considered a promising desalination technique for brackish water because of its high energy efficiency, easy operation, and eco-friendly process.[1-6] In principle, CDI requires pairs of inactive materials having a high surface area, in which the electrodes are oppositely positioned. As the saltwater flows between the electrodes, ions are harvested and stored in an electrical double layer by applying a potential across the layer. This phenomenon is similar to the principle of a double layer capacitor (EDLC), a common energy storage system.[7-11]

However, CDI has limitations in desalting highly concentrated feed water because the capacity is not sufficient for harvesting ions, and for this reason increasing the desalination capacity is a key issue in the development of CDI systems.[7, 12, 13] To overcome this limitation, innovative desalination techniques based on capacitive systems such as membrane capacitive deionization (MCDI),[14-17] flow-through electrode capacitive desalination (FTE CD),[18] wires,[19] flow-electrode capacitive deionization (FCDI),[20] and batteries[21-23] have been reported.

MCDI is a system in which cation and anion exchange membranes are added between two porous carbon electrodes. As a result, it has both a higher efficiency and salt removal rate compared to CDI.[14-17] In the FTE CD system, feed water flows through a porous carbon architecture, and the ion adsorption rate is significantly increased compared to a typical CDI system.[18] A wire-based capacitive system consists of wire electrode pairs; in this system, deionized water is produced as a continuous stream during the desalination process.[19] FCDI is a novel CDI system that uses a flow-electrode in which the carbon suspension flows on the surface of the current collectors. In this system, no discharge step is required in order to release the ions captured during the charging step in the same cell, and the scale-up of FCDI is easier than for a typical CDI system.[20] However, though these novel desalination techniques have good performance and high efficiency, the desalination capacity is still limited by the use of carbon materials, i.e., these systems require an abundant supply of carbon materials to treat highly concentrated feed water.

Another innovative desalination technique is a battery-based desalination process,[21-24] in which the electrodes are composed of battery materials. In this system, ions are captured by chemical bonds instead of the electrical double layer in the CDI system. This method is expected to have a high desalination capacity and ion selectivity because the battery materials themselves have a high specific capacity and unique structure. Note that, to date, although the system has shown a high efficiency and desalination capacity, the performance rate of its desalination process is slower than current CDI systems.
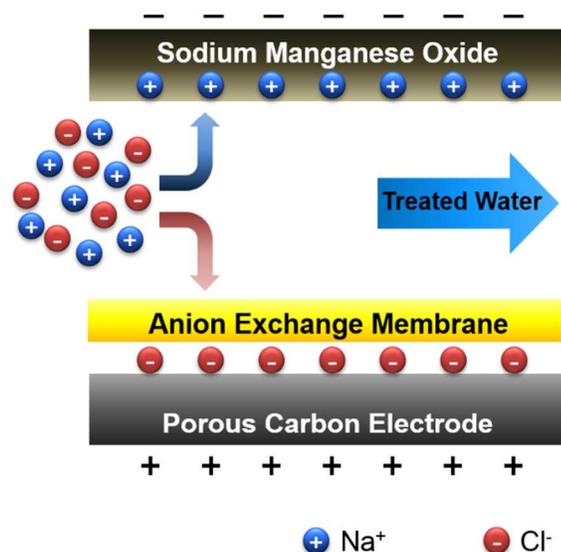
Fig. 1 Schematic diagram of desalination via HCDI. The HCDI system consists of an NMO electrode, anion exchange membrane, and porous carbon electrode. When a cell voltage is applied between the NMO and carbon electrodes, sodium ions are held by the chemical reaction in the NMO electrode, whereas chloride ions are held in the electric double layers formed at the surface of the porous carbon electrode.

In this study, we propose a new method to desalt water by combining CDI and battery systems to increase the desalination performance of capacitive techniques, referred to here as "hybrid capacitive deionization (HCDI)". This concept is shown in Fig. 1. HCDI is an asymmetric system that contains a sodium manganese oxide (NMO) electrode, an anion exchange membrane, and a porous carbon electrode. During the desalination process, sodium ions are held by the chemical reaction in the NMO electrode, whereas chloride ions are held in the electric double layers formed at the surface of the porous carbon electrode. In this work, we present how the desalination performance of the HCDI is improved by using sodium manganese oxide and activated carbon electrodes.

Experimental Section

Material synthesis

The sodium manganese oxide (NMO) used in this study was synthesized using a solid-state reaction. To make $Na_4Mn_9O_{18}$, Mn_2O_3 (Aldrich) was ball-milled with Na_2CO_3 (Aldrich) at a molar ratio of 0.484: 1 (Na_2CO_3:Mn_2O_3). The precursor mix was heated at 500 °C for 5 h under air conditioning; the resulting production was ball-milled again and heated at 900 °C for 12 h under air. The results of the NMO powder were characterized using X-ray powder diffraction (XRD, D8 Discover), and scanning electron microscopy (SEM, FESEM, JEOL JSM 6700 F) image are provided in the Electronic Supplementary Information (see ESI Fig. S1).

Electrode fabrication

The NMO and activated carbon electrodes were prepared as follows. Synthesized $Na_4Mn_9O_{18}$ powder or activated carbon (MSP-20, Kansai Coke and Chemicals), carbon black (Super P, Timcal Graphite and Carbon) as a conducting agent, and polytetrafluoroethylene (PTFE, Sigma-Aldrich) added as a binder (86:7:7 weight ratio) were mixed in ethanol to obtain a slurry mixture. After the resulting slurry was mixed for 30 min, it was rolled using a roll press machine to make sheet-type electrodes having a 300 μm thickness. The fabricated electrodes were dried in a vacuum oven at 60 °C for 12 h to remove any remaining solvent.

Electrochemical characterization of the electrodes

Cyclic voltammetry and galvanostatic charging/discharging were performed to examine the electrochemical properties of the NMO and activated carbon electrodes using a potentiostat/galvanostat (PARSTAT 2273, Princeton Applied Research) and a battery cycler (WBCS3000, WonA Tech Co.). Cyclic voltammetry were conducted using a three-electrode system, in conjunction with a 1 M aqueous NaCl solution. The NMO and activated carbon electrodes were used as the working electrodes, a platinum mesh electrode was employed as the counter electrode, and a KCl-saturated Ag/AgCl electrode was used as the reference electrode.

Galvanostatic charge/discharge tests were conducted on the two activated carbon electrodes and the NMO/activated carbon cell (d = 18 mm). The cell was a two-electrode system, and a cellulose nitrate membrane (thickness ~110 μm, Advanced Microdevice) was used as the separator. The cycling ability of the NMO/activated carbon cell was measured at a current density of 10 mA/cm^2 at a potential window of 0.0–0.8 V in a 1 M aqueous NaCl solution.

Desalination performance test

The desalination performance of HCDI was examined in a CDI module, as shown in Fig. 2. The HCDI module cell was composed of a NMO electrode (d = 50 mm, 670 ± 30 mg), nylon spacer (thickness: 200 μm), an anion exchange membrane (AMV, AGC engineering Co.), and an activated carbon electrode (d = 50 mm, 330 ± 10 mg). Before the desalination performance test, 0.8 V (*vs*. Ag/AgCl) was applied to the NMO electrode for 60 min to extract sodium ions from the NMO electrode. The contact area of the cell was 19.6 cm2, and graphite sheets were used as current collectors.

To investigate the treatment performance of various operation conditions in the HCDI system, different concentrations of source water and voltages were employed. The source water was varied from 5 mM to 100 mM NaCl at a flow rate of 10 mL/min; the ion removal test was initiated from the charging step, in which adsorption was achieved by applying a voltage (0.8 V to 1.2 V) for 15 min using a battery cycler (WBC S3000, WonA Tech Co.). After that, the captured ions were released by applying a negative voltage (-0.8 V to -1.2 V) for 15 min. During the test, the effluent conductivity was measured using a flow-type conductivity meter (3573-10C, HORIBA). The accumulated ion removal capacity was then
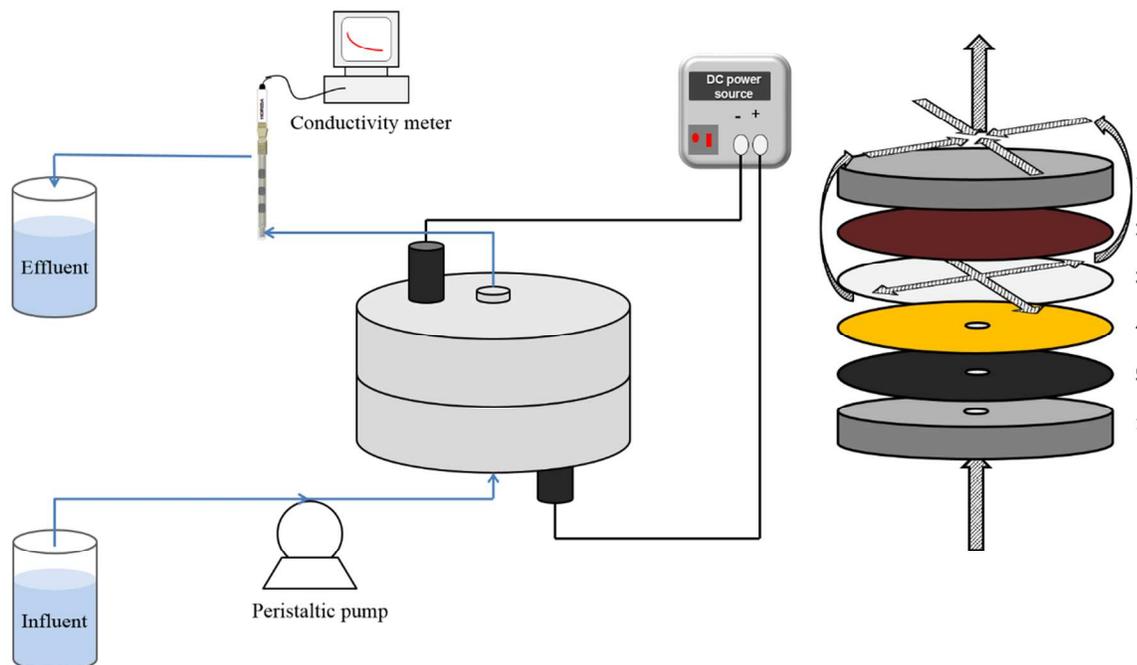
Fig. 2 Schematic diagram of the HCDI module for the desalination performance test (1: graphite sheet current collector, 2. NMO electrode, 3. nylon spacer, 4. anion exchange membrane, 5. activated carbon electrode).

expressed as the deionized NaCl mass per total weight of NMO and activated carbon electrodes during the ion removal step. The captured NaCl was calculated from the concentration change in the effluent measured by the conductivity meter. The representative results from duplicate or triplicate experiments are presented in this work.

Results and Discussion

Fig. 3(a) and (b) shows the conductivity changes of the HCDI system during the ion capture/release step in a 10 mM NaCl aqueous solution and the current profiles during operation. The conductivity changes indicate that the HCDI system successfully captured and released ions, and it was reproducible for each cycle. The initial conductivity of the effluent rapidly decreased as a result of quick intercalation and adsorption; sodium ions were intercalated into the NMO electrode, and chloride ions were adsorbed onto the surface of the activated carbon electrode. The current profiles during the operation show similar properties of constant voltage operation in CDI or MCDI, which indicates that the current is mainly related to the ions captured and released during operation.[1, 3, 5, 11] Note that in the HCDI system, an anion selective membrane was placed on the carbon electrode to prevent the adsorption of cations onto the carbon electrode since cations in the solution can be adsorbed on the surface of the carbon electrode during operation, which would decrease the efficiency of the desalination performance.[15-17] Compared to the carbon electrode, however, no ion selective membrane was required for the NMO electrode because manganese oxide-based materials

selectively react with cations.[21,24,25] Fig. 3(c) shows the time-dependent accumulated ion removal capacity and ion removal rate. The accumulated ion removal capacity is given by the integral of conductivity changes during the third ion-capturing step. The ion removal capacity during the 15 min ion capturing process was 31.2 mg/g, expressed as the mass of deionized ionic charge per the total mass of the NMO and activated carbon electrode. This capacity is more than two times higher than a standard CDI system (13.5 mg/g), and even higher than the MCDI system in our group (22.4 mg/g) based on the same reactor and activated carbon electrode (see ESI Fig. S3). The accumulated ion removal rate, which is a performance indicator of rate in CDI systems, is given by the accumulated mass of deionized sodium chloride ions (mg) per total electrode mass (g) divided by the operation time (s); this parameter is a similar to the average salt adsorption rate (ASAR) reported by Zhao *et al.*[26] for CDI systems. The maximum ion removal rate can be calculated from the peak of curves; the rate attained here was 0.066 mg NaCl per g of electrodes per second. It is an excellent value compared to the results of a CDI system using the same activated carbon electrode (0.048 mg/g/s). Compared to an MCDI system (0.072 mg/g/s), the performance per electrode mass was slightly lower; however, it remains remarkable when considering the active cell area instead of the total electrodes mass (HCDI: 0.0033 mg/cm^2/s, MCDI: 0.0025 mg/cm^2/s).

To investigate the performance of the HCDI system at various operation conditions, different voltages and concentrations of NaCl solution were employed. Fig. 4(a) and (b) present the results of the ion removal performance at different voltages in a 10 mM NaCl solution. The ion removal
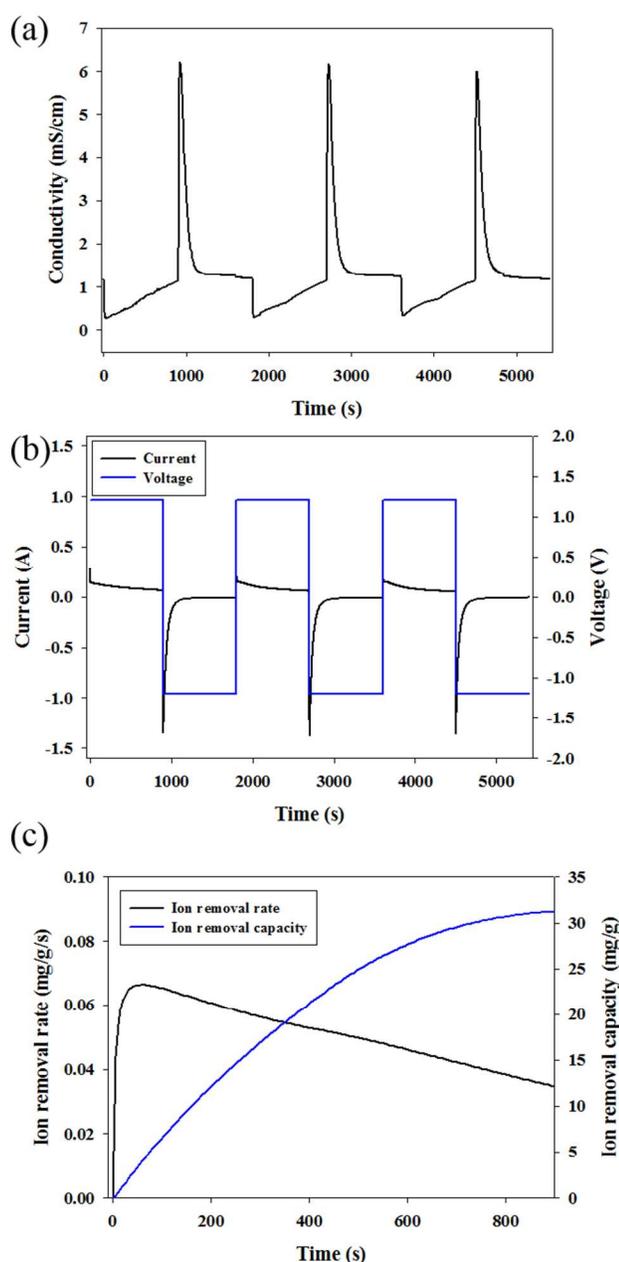
Fig. 3 Representative desalination performance of the HCDI system. (a) The conductivity changes of the effluent during 3 cycles. The operation was carried out in 10 mM NaCl (1.2 V for 15 min during the ion-capturing step, and -1.2 V for 15 min during the ion-releasing step). (b) Current and voltage profiles during operation. (c) Ion removal capacity and accumulated ion removal rate of HCDI during the third ion capturing step, represented as the mass of deionized ionic charge (mg) per the total mass of the NMO and activated carbon electrodes (g).
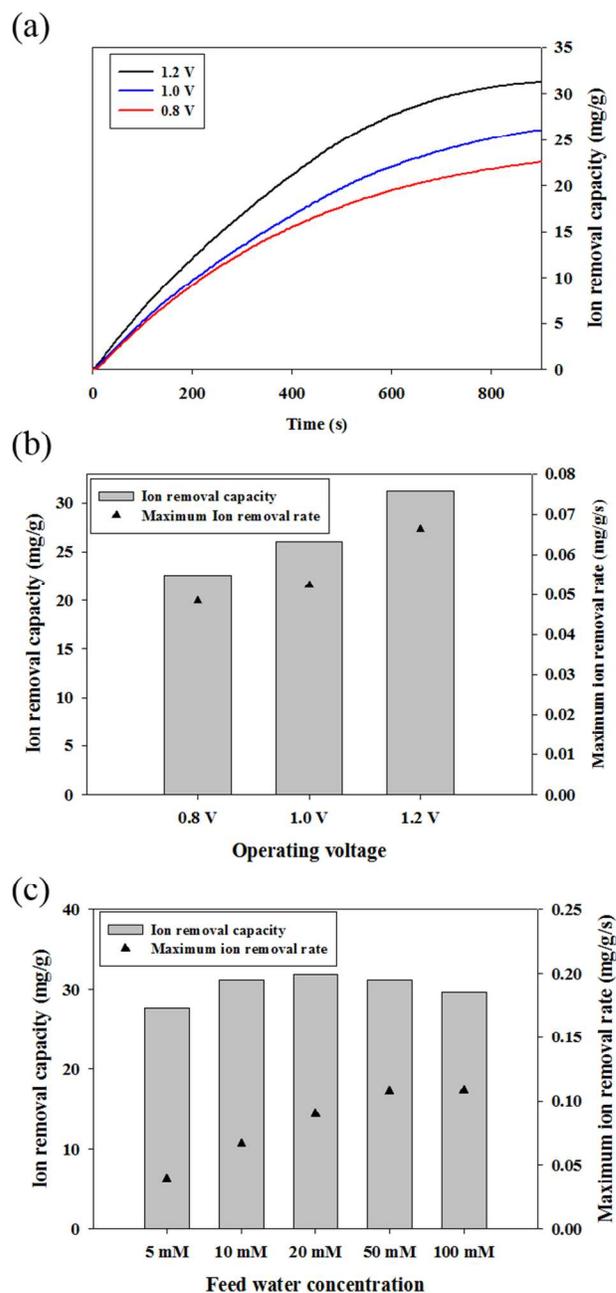
Fig. 4 (a) Ion removal capacity of HCDI at different voltage operations in 10 mM NaCl solution (0.8 V to 1.2 V for 15 min during the ion-capturing step, and -0.8 V to -1.2 V for 15 min during the ion-releasing step). (b) Ion removal capacity and maximum ion removal rate at different voltage operations, and (c) various concentrations of NaCl solution (1.2 V for 15 min during the ion-capturing step, and -1.2 V for 15 min during the ion-releasing step).

capacity of HCDI at 0.8 V, 1.0 V, and 1.2 V applied voltages were 22.6 mg/g, 26.1 mg/g, and 31.2 mg/g, respectively. As the results show, the ion removal capacity and rate increased as the applied voltage was increased from 0.8 V to 1.2 V. These increases are due to the increase in the electrosorptive capacity of activated carbon electrode and the reaction rate in NMO electrodes when a higher voltage is applied.[1, 3, 5] The effect of

effluent concentration on the HCDI system was also investigated (Fig. 4(c)), to reveal the ion removal capacity and maximum ion removal rate of HCDI with respect to various NaCl concentrations. For initial salt concentrations of 5 mM, 10 mM, 20 mM, 50 mM, and 100 mM, the ion removal capacities were 27.7 mg/g, 31.2 mg/g, 31.9 mg/g, 31.2 mg/g, and 29.6 mg/g, respectively. These results imply that the ion removal

capacity of an HCDI system has similar performances for various concentrations, and that this system can be applied to desalting NaCl solutions having a wide concentration range. To apply the HCDI system to actual brackish water, an additional test is presented in the in the Electronic Supplementary Information, using simulated brackish water in which the chemical composition was similar with water obtained from natural gas operation, and the results indicate that the HCDI system can be applied to treat brackish water (see ESI Table S1).[27] The maximum ion removal rate exhibited an increase over the initial salt concentration at the range of 5 mM to 20 mM, and maintained this performance when the salt concentration was higher than 20 mM. This behavior indicates that a higher initial salt concentration reduces the total resistance of the HCDI cell. As a result, it leads to a rapid chemical reaction and adsorption during the early phase of the ion removal operation for a source water concentration below 20 mM. However, there is a limit to how much the maximum ion removal rate can be increased by reducing the resistance of electrolyte.

Fig. 5(a) and (b) present the results of cyclic voltammetry for the NMO and activated carbon electrode. The CV measurement for the NMO electrode was performed at a scan rate of 2 mV/s (0 V to 0.8 V *vs*. Ag/AgCl) in a three-electrode system, using a platinum mesh as the counter electrode. In Fig. 5(a), intercalation and deintercalation peaks that have been reported in previous studies were observed.[28, 29] The NMO electrode has excellent stability in an aqueous solution, with
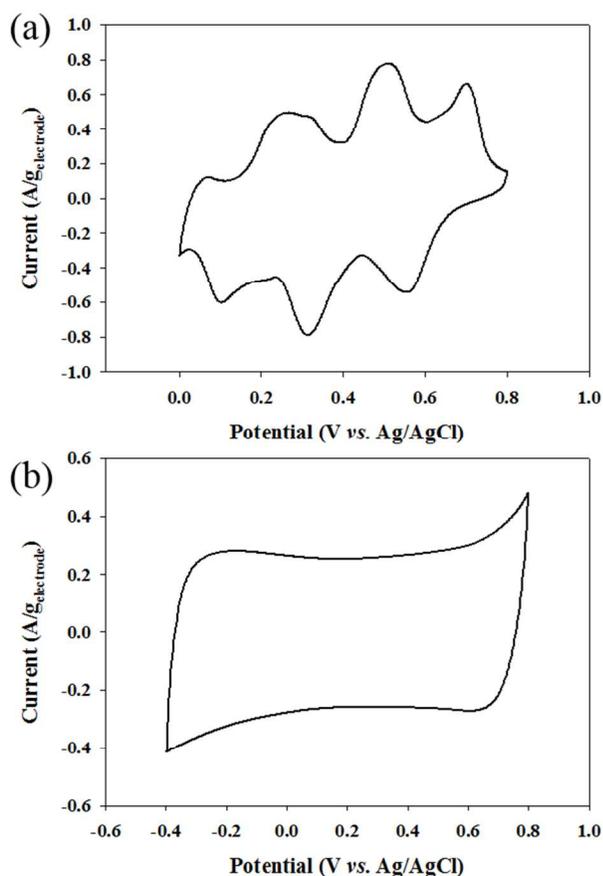

Fig. 5 Cyclic voltammetry (2 mV/s) for: (a) NMO ($Na_4Mn_9O_{18}$) electrode, and (b) activated carbon electrode (MSP-20) in 1 M NaCl.

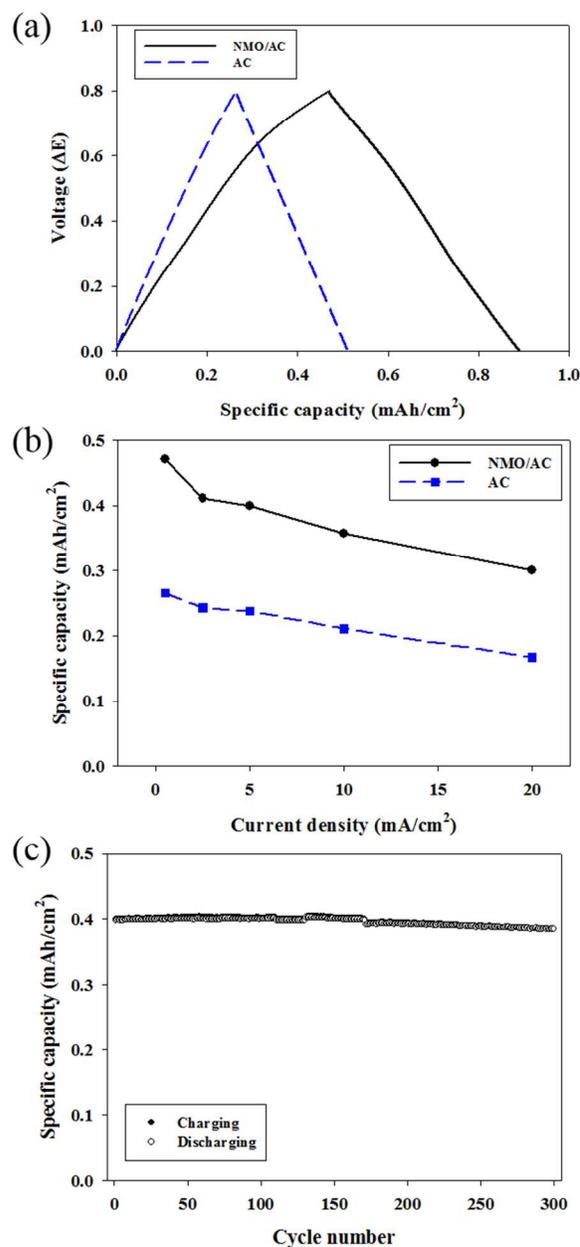**Fig. 6** (a) Charge/discharge data (i = 0.5 mA/cm²) and (b) specific capacity at different current densities of NMO/AC (MSP-20) and symmetric activated carbon (MSP-20) system in 1 M NaCl. (c) Cell charge and discharge capacity retention of an NMO/AC carbon system as a function of the cycle number (10 mA/cm² galvanostatic cycling with a potential window of 0.0 V to 0.8 V).

high capacity, and there have been successful demonstrations in aqueous Na-ion batteries for positive electrode materials.[30, 31, 33, 34] Fig. 5(b) shows a cyclic voltammogram collected from an activated carbon electrode (MSP-20) within a potential window of -0.4 V to 0.8 V (*vs*. Ag/AgCl). The cyclic voltammetry curve exhibits a rectangular shape, which is a typical charge/discharge voltammogram of a capacitor. In the HCDI system, chloride ions can move through the anion exchange membrane and adsorb onto the surface of the activated carbon

electrode when a positive potential is applied. In contrast, chloride ions desorb from the activated carbon electrode during the ion-releasing step.

Fig. 6(a) and (b) show the galvanostatic performance of activated carbon and NMO/activated carbon systems at a current density of 0.5 mA/cm^2 and 0.5 mA/cm^2 to 20 mA/cm^2 galvanostatic cycling, for a potential window of 0.0 V to 0.8 V in a 1 M NaCl aqueous solution. For the NMO/activated carbon system, the NMO electrode used a positive electrode. From the data, we observed that the asymmetric system had a higher capacity than the symmetric activated carbon system in the same cell area, and that the asymmetric system maintained a high capacity at different current densities. These results have been previously reported for a hybrid capacitor, which is an energy storage system that combines a supercapacitor and battery electrode.[30, 31] In most literature, $Na_4Mn_9O_{18}$ has a large charge capacity (40 mAh/g to 50 mAh/g), and this value corresponds to a capacitance of more than 300 F/g, which is higher than for activated carbon materials.[28] $Na_4Mn_9O_{18}$ is known to have a high performance rate for sodium ion diffusion in aqueous electrolytes because it has plenty of vacancies in its S-shaped tunnel, and thus the structure delivers a rapid diffusion and phase transition of sodium ions.[32, 33] This characteristic of $Na_4Mn_9O_{18}$ leads to the high capacity and performance rate seen in the desalination performance and Fig. 6(b) results, even though the NMO electrode is as thick as the activated carbon electrode (300 μm). The galvanostatic cycling performance of the NMO/AC cell is shown in Fig. 6(c), in which the cell charged and discharged between 0.0 V to 0.8 V at a current density of 10 mA/cm^2 in a 1 M NaCl solution. As the figure shows, the charge/discharge capacity indicates excellent capacity retention during cycling, having a columbic efficiency of nearly 100% though 300 cycles. This result suggests that the electrochemical performance of the NMO/AC asymmetric system is stable, and that it can be used repetitively in an aqueous NaCl solution.

Conclusions

This study describes an HCDI system, which is a novel desalination technique based on a capacitive system that combines a battery and activated carbon materials. The HCDI system successfully desalted a high capacity sodium chloride solution (31.2 mg/g), compared to a CDI system (13.5 mg/g). Moreover, it was found that the system had a rapid ion removal rate and excellent stability in an aqueous sodium chloride solution. Thus, it could be concluded that the HCDI system improved the desalination performance of a CDI system, and as such it could be a feasible method for treating highly concentrated feed water.

Acknowledgements

Notes and references

^{a} School of Chemical and Biological Engineering, College of Engineering, Institute of Chemical Process, Seoul National University (SNU), Daehak-dong, Gwanak-gu, Seoul 151-742, Republic of Korea, Fax: +82-2-876-8911; Tel: +82-2-880-8941; E-mail: jeyong@snu.ac.kr

1. J. C. Farmer, D. V. Fix, G. V. Mack, R. W. Pekala and J. F. Poco, *J. Electrochem. Soc.*, 1996, **143**, 159-169.
2. M. A. Anderson, A. L. Cudero and J. Palma, *Electrochim. Acta*, 2010, **55**, 3845-3856.
3. J.-H. Lee, W.-S. Bae and J.-H. Choi, *Desalination*, 2010, **258**, 159-163.
4. S.-J. Seo, H. Jeon, J. K. Lee, G.-Y. Kim, D. Park, H. Nojima, J. Lee and S.-H. Moon, *Water Res.*, 2010, **44**, 2267-2275.
5. Y. Bouhadana, E. Avraham, M. Noked, M. Ben-Tzion, A. Soffer and D. Aurbach, *J. Phys. Chem. C*, 2011, **115**, 16567-16573.
6. P. Xu, J. E. Drewes, D. Heil and G. Wang, *Water Res.*, 2008, **42**, 2605-2617.
7. M. Noked, A. Soffer and D. Aurbach, *J. Solid State Electrochem.*, 2011, **15**, 1563-1578.
8. C. Kim, J. Lee, S. Kim and J. Yoon, *Desalination*, 2014, **342**, 70-74.
9. T. Kim and J. Yoon, *J. Electroanal. Chem.*, 2013, **704**, 169-174.
10. S. Porada, L. Borchardt, M. Oschatz, M. Bryjak, J. Atchison, K. Keesman, S. Kaskel, P. Biesheuvel and V. Presser, *Energy Environ. Sci.*, 2013, **6**, 3700-3712.
11. S. Porada, R. Zhao, A. Van Der Wal, V. Presser and P. Biesheuvel, *Prog. Mater. Sci.*, 2013, **58**, 1388-1442.
12. C. Tsouris, R. Mayes, J. Kiggans, K. Sharma, S. Yiacoumi, D. DePaoli and S. Dai, *Environ. Sci. Technol.*, 2011, **45**, 10243-10249.
13. X. Wen, D. Zhang, L. Shi, T. Yan, H. Wang and J. Zhang, *J. Mater. Chem.*, 2012, **22**, 23835-23844.
14. J.-B. Lee, K.-K. Park, H.-M. Eum and C.-W. Lee, *Desalination*, 2006, **196**, 125-134.
15. P. Biesheuvel and A. Van der Wal, *J. Membr. Sci.*, 2010, **346**, 256-262.
16. J.-Y. Lee, S.-J. Seo, S.-H. Yun and S.-H. Moon, *Water Res.*, 2011, **45**, 5375-5380.
17. H. Li and L. Zou, *Desalination*, 2011, **275**, 62-66.
18. M. E. Suss, T. F. Baumann, W. L. Bourcier, C. M. Spadaccini, K. A. Rose, J. G. Santiago and M. Stadermann, *Energy Environ. Sci.*, 2012, **5**, 9511-9519.
19. S. Porada, B. Sales, H. Hamelers and P. Biesheuvel, *J. Phys. Chem. Lett.*, 2012, **3**, 1613-1618.
20. S.-i. Jeon, H.-r. Park, J.-g. Yeo, S. Yang, C. H. Cho, M. H. Han and D.-K. Kim, *Energy Environ. Sci.*, 2013, **6**, 1471-1475.
21. F. La Mantia, M. Pasta, H. D. Deshazer, B. E. Logan and Y. Cui, *Nano Lett.*, 2011, **11**, 1810-1813.

22. M. Pasta, C. D. Wessells, Y. Cui and F. La Mantia, *Nano Lett.,* 2012, **12**, 839-843.

23. M. Pasta, A. Battistel and F. La Mantia, *Energy Environ. Sci.*, 2012, **5**, 9487-9491.

24. J. Lee, S.-H. Yu, C. Kim, Y.-E. Sung and J. Yoon, *Phys. Chem. Chem. Phys.*, 2013, **15**, 7690-7695.

25. M. Jayalakshmi, M. Mohan Rao and F. Scholz, *Langmuir*, 2003, **19**, 8403-8408.

26. C. Xu, H. Du, B. Li, F. Kang and Y. Zeng*, J. Electrochem. Soc.*, 2009, **156**, A73-A78.

27. R. Zhao, O. Satpradit, H. H. M. Rijnaarts, P. M. Biesheuvel and A. van der Wal, *Water Res.*, 2013, **47**, 1941-1952.

28. R. Xu, J. E. Drewes, D. Heil and G. Wang, *Water Res.*, 2008, **42**, 2605-2617.

29. J. Whitacre, A. Tevar and S. Sharma, *Electrochem. Commun.*, 2010, **12**, 463-466.

30. X. Liu, N. Zhang, J. Ni and L. Gao, *J. Solid State Electrochem.*, 2013, **17**, 1939-1944.

31. M. S. Hong, S. H. Lee and S. W. Kim, *Electrochem. Solid-State Lett.*, 2002, **5**, A227-A230.

32. J. H. Park, O. O. Park, K. H. Shin, C. S. Jin and J. H. Kim, *Electrochem. Solid-State Lett.*, 2002, **5**, H7-H10.

33. Z. Li, D. Young, K. Xiang, W. C. Carter and Y. M. Chiang, *Adv. Energy Mater.*, 2013, **3**, 290-294.

34. D. J. Kim, R. Ponraj, A. G. Kannan, H.-W. Lee, R. Fathi, R. Ruffo, C. M. Mari and D. K. Kim, *J. Power Sources*, 2013, **244**, 758-763.